

Anisotropic elasticity of multilayered crystals deformed by a biperiodic network of misfit dislocations

X. Wang,¹ E. Pan,¹ and J. D. Albrecht²¹*Department of Engineering and Department of Applied Mathematics, University of Akron, Akron, Ohio 44325-3905, USA*²*Air Force Research Laboratory, Wright-Patterson Air Force Base, Ohio 45433, USA*

(Received 30 May 2007; revised manuscript received 10 August 2007; published 24 October 2007)

We investigate the displacement and stress fields associated with a biperiodic misfit dislocation network located along a single interface in a multilayered crystal composite of $(N-1)$ thin bonded anisotropic elastic layers sandwiched between two semi-infinite anisotropic media. Specifically, dislocation networks of coplanar, biperiodic, hexagonal-based linear misfit are considered within continuum elasticity theory. While the homogeneous solutions are obtained by using the double Fourier series and the Stroh formalism, the solutions for multilayered structures are expressed in terms of a transfer matrix technique and the generalized Barnett-Lothe tensors. The transfer matrix technique lends itself to composites containing large numbers of bonded crystal layers because only a 3×3 matrix inversion is required. The use of the generalized Barnett-Lothe tensor facilitates the treatment of inherent elastic anisotropy in the constituent crystals. The correctness and the versatility of the method are illustrated by calculating the stress field associated with a multilayer formed by alternating GaAs and Si layers ($N=5$) containing a single array of edge misfit dislocations along one interface. To further demonstrate the influence of the material anisotropy, numerical examples for the misfit dislocation induced stresses are given for the ($N=5$) multilayered structure (formed by GaAs and Si) and for the induced surface displacements for an InAs thin film over a GaAs substrate. Both cubic and simplified isotropic materials are considered.

DOI: [10.1103/PhysRevB.76.134112](https://doi.org/10.1103/PhysRevB.76.134112)

PACS number(s): 61.72.Ff, 68.55.Ln, 68.47.Fg, 62.20.Dc

I. INTRODUCTION

The exploration of dissimilar semiconductor heterostructures that are far beyond the limits of typical pseudomorphic (or coherent) epitaxy is being considered in order to provide greater functionality and configuration of highly integrated electronic and optoelectronic microsystems.¹ One structural approach is the bonding² of mismatched semiconductors such as Si and GaAs that require structural defects to accommodate the strain at the interfaces.

Multilayered structures made of ultrathin lamellae exhibit excellent mechanical properties, such as higher yield strength, higher ductility and toughness, and creep resistance.³⁻⁶ Periodic arrays of defects, such as dislocations, have been observed along the interfaces, which can enhance the macroscopic properties of the composite material.⁶ Periodic boundary conditions are ubiquitous in describing crystalline states theoretically and computationally.^{7,8} In this paper, we develop a theoretical framework that accounts for the elastic properties of observed periodic dislocation arrays in multilayered structures.

The elastic fields for a multilayered composite containing one periodic (or biperiodic) array of interfacial misfit dislocations have been investigated by using Fourier or double Fourier series expansion methods.⁹⁻¹⁴ However, this method is limited and time consuming as it requires the inversion of a $6N \times 6N$ matrix for a laminated medium containing N interfaces. This is especially problematic when N is very large (say, $N=100, 1000,$ or $10\,000$), not to mention that the inversion of the $6N \times 6N$ matrix is only for one term in the Fourier or double Fourier series. Therefore, the cost of complete solutions by taking sufficiently large number of the Fourier or double Fourier series would be formidable. Due to

the computational demands, previous calculations have been restricted to treating the elastic fields of isotropic or anisotropic two-layer systems deformed by a biperiodic network of misfit dislocations.¹²⁻¹⁴ Even for the simpler two-dimensional (2D) problem of periodic misfit dislocations, only the elastic field for layered structures containing a few layers has been calculated.^{9,10} Based on published reports, we concluded that the elasticity associated with a multilayered crystal system containing a biperiodic array of interfacial misfit dislocations is still far from complete.

In this research, we propose an efficient method based on the Stroh formalism¹⁵⁻¹⁷ and transfer matrix¹⁷⁻¹⁹ techniques to investigate the displacement and stress fields associated with a biperiodic, hexagonal-based misfit dislocation network located along one planar interface in an anisotropic and multilayered crystal composite. It will be found that by utilizing the present approach, we can address a multilayered crystal composed of an arbitrary number of anisotropic (or isotropic) elastic layers.

II. SPECIFICATION OF THE PROBLEM

We consider the deformation of a multilayered structure composed of a stack of $(N-1)$ thin bonded anisotropic elastic layers, sandwiched between two semi-infinite anisotropic media denoted 1 and $(N+1)$, as shown in Fig. 1. A Cartesian coordinate system (x_1, x_2, x_3) is established in such a way that the bottom interface is at $x_3=0$ and the top interface is at $x_3=H$, where H is the total thickness of the $(N-1)$ thin anisotropic elastic layers. The homogeneous and anisotropic elastic thin layer k ($2 \leq k \leq N$) is bounded by its lower interface at $x_3=z_{k-1}$ and upper interface at $x_3=z_k$ with its thick-

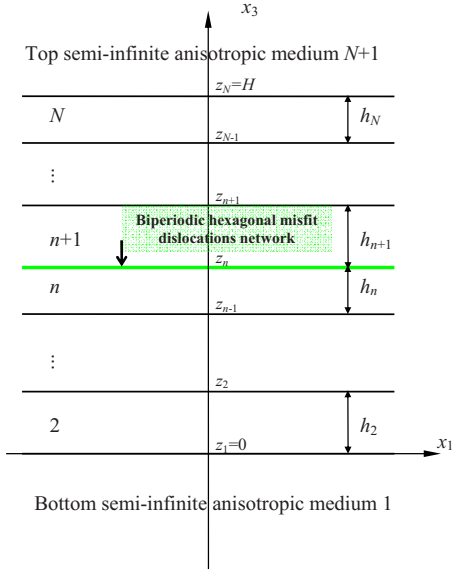


FIG. 1. (Color online) Cross section of a multilayered system with N interfaces and $(N+1)$ anisotropic elastic media. A bipерiodic, hexagonal, misfit dislocation network that accommodates a misfit dislocation between layer n and layer $n+1$ lies on the interface $x_3 = z_n$ of the multilayered structure.

ness $h_k = z_k - z_{k-1}$, and the layers are numbered sequentially starting at 2 from the bottom thin layer. Apparently, $z_N = H = \sum_{k=2}^N h_k$. A bipерiodic, hexagonal misfit dislocation network that accommodates a lattice misfit between layer n and layer $n+1$ lies on the interface $x_3 = z_n$. The following boundary conditions are assumed: (i) except for the interface at $x_3 = z_n$ between layer n and layer $n+1$, perfect bonding conditions exist between any two adjacent elastic media; (ii) continuity condition of tractions across the interface $x_3 = z_n$; (iii) linear variations of the relative interface displacement field across the interface $x_3 = z_n$ inside each bipерiodic pattern of misfit dislocations.^{12,14} The multilayered structure discussed in this paper is general in the sense that if we let the elastic constants of the bottom (or top) semi-infinite medium be very small, the multilayered system is then built with a package of $(N-1)$ thin bonded layers with a traction-free surface at $x_3 = 0$ (or $x_3 = H$), bounded by a semi-infinite medium. Furthermore, if we let the elastic constants of both the two semi-infinite media be very small, the multilayered system is then made of a package of $(N-1)$ thin bonded layers with two traction-free surfaces at $x_3 = 0$ and $x_3 = z_N$.

The displacement jumps across the interface $x_3 = z_n$ can be expanded into a bipерiodic Fourier series as^{12,14}

$$[u_k^+ - u_k^-]_{x_3=z_n} = \Delta_k^{(\mathbf{G}=0)} + \sum_{\mathbf{G} \neq 0} \Delta_k^{(\mathbf{G})} e^{2\pi i(G_1 x_1 + G_2 x_2)}, \quad (1)$$

which describes a function depending linearly on x_1 and x_2 inside the domain considered. In Eq. (1), \mathbf{G} is a reciprocal vector of the 2D lattice defined by the two periodic vectors \mathbf{a} and \mathbf{c} . If n and m are integers, then $\mathbf{G} = n\mathbf{a}^* + m\mathbf{c}^*$ in terms of the base vectors.¹³ The components of \mathbf{G} with respect to the Cartesian coordinate system are $(G_1, G_2, 0)$. (It should be mentioned for clarity that we employ a different coordinate

system than that adopted in Refs. 12–14.) The specific expressions of the coefficients $\Delta_k^{(\mathbf{G})}$ have been given in other works.^{12,14} In addition, we can further take $\Delta_k^{(\mathbf{G}=0)} = 0$ to enforce that the displacements are continuous at $x_1 = x_2 = 0$, $x_3 = z_n$.

III. STROH FORMALISM FOR BIPERIODIC PROBLEMS

In this section, we first derive the expressions of displacement and stress fields in any homogeneous and anisotropic elastic layer by invoking the established Stroh formalism.

The linear constitutive equations, strain-displacement equations, and equilibrium equations in the absence of body force can be expressed as¹⁶

$$\sigma_{ij} = c_{ijkl} \varepsilon_{ij}, \quad (2a)$$

$$\varepsilon_{ij} = \frac{1}{2}(u_{i,j} + u_{j,i}), \quad (2b)$$

$$\sigma_{ij,j} = 0, \quad (2c)$$

where σ_{ij} , ε_{ij} , and u_i are, respectively, the stress, strain, and displacement, and c_{ijkl} are the elastic moduli.

For a certain nonzero \mathbf{G} , we seek the solution of the displacement vector in the form

$$\mathbf{u} = \begin{bmatrix} u_1 \\ u_2 \\ u_3 \end{bmatrix} = e^{i(k_1 x_1 + k_2 x_2 + p x_3)} \begin{bmatrix} a_1 \\ a_2 \\ a_3 \end{bmatrix}, \quad (3)$$

where p and a_i ($i=1-3$) are unknowns, and

$$k_1 = 2\pi G_1, \quad k_2 = 2\pi G_2 \quad (G_1^2 + G_2^2 \neq 0). \quad (4)$$

Substitution of Eq. (3) into the strain-displacement relation [Eq. (2b)] and subsequently into the constitutive relation Eq. (2a) yields the traction vector (at $x_3 = \text{constant}$) as

$$\mathbf{t} = \begin{bmatrix} \sigma_{13} \\ \sigma_{23} \\ \sigma_{33} \end{bmatrix} = i e^{i(k_1 x_1 + k_2 x_2 + p x_3)} \begin{bmatrix} b_1 \\ b_2 \\ b_3 \end{bmatrix}. \quad (5)$$

If we introduce two vectors

$$\mathbf{a} = [a_1 \ a_2 \ a_3]^T, \quad \mathbf{b} = [b_1 \ b_2 \ b_3]^T, \quad (6)$$

then it is found that vector \mathbf{b} is related to vector \mathbf{a} through

$$\mathbf{b} = (\mathbf{R}^T + p\mathbf{T})\mathbf{a} = -\frac{1}{p}(\mathbf{Q} + p\mathbf{R})\mathbf{a}, \quad (7)$$

where the superscript T denotes the matrix transpose and \mathbf{Q} , \mathbf{T} , \mathbf{R} are three 3×3 real matrices defined by

$$\mathbf{Q} = \mathbf{Q}^T = \begin{bmatrix} k_1^2 c_{11} + 2k_1 k_2 c_{16} + k_2^2 c_{66} & k_1^2 c_{16} + k_1 k_2 (c_{12} + c_{66}) + k_2^2 c_{26} & k_1^2 c_{15} + k_1 k_2 (c_{14} + c_{56}) + k_2^2 c_{46} \\ k_1^2 c_{16} + k_1 k_2 (c_{12} + c_{66}) + k_2^2 c_{26} & k_1^2 c_{66} + 2k_1 k_2 c_{26} + k_2^2 c_{22} & k_1^2 c_{56} + k_1 k_2 (c_{25} + c_{46}) + k_2^2 c_{24} \\ k_1^2 c_{15} + k_1 k_2 (c_{14} + c_{56}) + k_2^2 c_{46} & k_1^2 c_{56} + k_1 k_2 (c_{25} + c_{46}) + k_2^2 c_{24} & k_1^2 c_{55} + 2k_1 k_2 c_{45} + k_2^2 c_{44} \end{bmatrix},$$

$$\mathbf{T} = \mathbf{T}^T = \begin{bmatrix} c_{55} & c_{45} & c_{35} \\ c_{45} & c_{44} & c_{34} \\ c_{35} & c_{34} & c_{33} \end{bmatrix},$$

$$\mathbf{R} = \begin{bmatrix} k_1 c_{15} + k_2 c_{56} & k_1 c_{14} + k_2 c_{46} & k_1 c_{13} + k_2 c_{36} \\ k_1 c_{56} + k_2 c_{25} & k_1 c_{46} + k_2 c_{24} & k_1 c_{36} + k_2 c_{23} \\ k_1 c_{55} + k_2 c_{45} & k_1 c_{45} + k_2 c_{44} & k_1 c_{35} + k_2 c_{34} \end{bmatrix}, \quad (8)$$

where the standard contracted notations $c_{\alpha\beta}$ for the elastic moduli c_{ijkl} have been adopted.

In addition, the in-plane stresses can be expressed as

$$\begin{bmatrix} \sigma_{11} \\ \sigma_{22} \\ \sigma_{12} \end{bmatrix} = ie^{i(k_1 x_1 + k_2 x_2 + p x_3)} \begin{bmatrix} k_1 c_{11} + k_2 c_{16} + p c_{15} & k_1 c_{16} + k_2 c_{12} + p c_{14} & k_1 c_{15} + k_2 c_{14} + p c_{13} \\ k_1 c_{12} + k_2 c_{26} + p c_{25} & k_1 c_{26} + k_2 c_{22} + p c_{24} & k_1 c_{25} + k_2 c_{24} + p c_{23} \\ k_1 c_{16} + k_2 c_{66} + p c_{56} & k_1 c_{66} + k_2 c_{26} + p c_{46} & k_1 c_{56} + k_2 c_{46} + p c_{36} \end{bmatrix} \begin{bmatrix} a_1 \\ a_2 \\ a_3 \end{bmatrix}. \quad (9)$$

The stress components should satisfy the equilibrium equations [Eq. (2c)], which in terms of vector \mathbf{a} yields the following eigenequation:

$$\{\mathbf{Q} + p(\mathbf{R} + \mathbf{R}^T) + p^2 \mathbf{T}\} \mathbf{a} = \mathbf{0}. \quad (10)$$

It is observed that Eq. (10), derived for the biperiodic problem, is identical in structure to the Stroh formalism in terms of the 2D Fourier transform for three-dimensional (3D) problems.^{15–19} This agreement is somewhat expected given that the Fourier transform is a generalization of the Fourier series in the limit as the period of the Fourier series approaches infinity. With aid of Eq. (7), Eq. (10) can be recast

into the following standard eigenvalue problem:

$$\mathbf{N} \begin{bmatrix} \mathbf{a} \\ \mathbf{b} \end{bmatrix} = p \begin{bmatrix} \mathbf{a} \\ \mathbf{b} \end{bmatrix}, \quad (11)$$

where

$$\mathbf{N} = \begin{bmatrix} -\mathbf{T}^{-1} \mathbf{R}^T & \mathbf{T}^{-1} \\ -\mathbf{Q} + \mathbf{R} \mathbf{T}^{-1} \mathbf{R}^T & -\mathbf{R} \mathbf{T}^{-1} \end{bmatrix}. \quad (12)$$

We remark that, for any material anisotropy, the expression of the material matrix \mathbf{N} is explicit. For example, when the material is orthotropic, the explicit expression of \mathbf{N} is

$$\mathbf{N} = \begin{bmatrix} 0 & 0 & -k_1 & 1/c_{55} & 0 & 0 \\ 0 & 0 & -k_2 & 0 & 1/c_{44} & 0 \\ -k_1 c_{13}/c_{33} & -k_2 c_{23}/c_{33} & 0 & 0 & 0 & 1/c_{33} \\ -k_1^2 (c_{11} - c_{13}^2/c_{33}) - k_2^2 c_{66} & -k_1 k_2 (c_{12} + c_{66} - c_{13} c_{23}/c_{33}) & 0 & 0 & 0 & -k_1 c_{13}/c_{33} \\ -k_1 k_2 (c_{12} + c_{66} - c_{13} c_{23}/c_{33}) & -k_1^2 c_{66} - k_2^2 (c_{22} - c_{23}^2/c_{33}) & 0 & 0 & 0 & -k_2 c_{23}/c_{33} \\ 0 & 0 & 0 & -k_1 & -k_2 & 0 \end{bmatrix}. \quad (13)$$

Furthermore, if the material is isotropic, then \mathbf{N} is reduced to

$$\mathbf{N} = \begin{bmatrix} 0 & 0 & -k_1 \frac{2}{c_{11} - c_{12}} & 0 & 0 \\ 0 & 0 & -k_2 & 0 & \frac{2}{c_{11} - c_{12}} & 0 \\ -\frac{k_1 c_{12}}{c_{11}} & -\frac{k_2 c_{12}}{c_{11}} & 0 & 0 & 0 & \frac{1}{c_{11}} \\ -k_1^2 \frac{c_{11}^2 - c_{12}^2}{c_{11}} - k_2^2 \frac{c_{11} - c_{12}}{2} & -k_1 k_2 \frac{c_{11}^2 + c_{11} c_{12} - 2c_{12}^2}{2c_{11}} & 0 & 0 & 0 & -\frac{k_1 c_{12}}{c_{11}} \\ -k_1 k_2 \frac{c_{11}^2 + c_{11} c_{12} - 2c_{12}^2}{2c_{11}} & -k_1^2 \frac{c_{11} - c_{12}}{2} - k_2^2 \frac{c_{11}^2 - c_{12}^2}{c_{11}} & 0 & 0 & 0 & -\frac{k_2 c_{12}}{c_{11}} \\ 0 & 0 & 0 & -k_1 & -k_2 & 0 \end{bmatrix}, \quad (14)$$

where $c_{11} = 2\mu(1-\nu)/(1-2\nu)$ and $c_{12} = 2\mu\nu/(1-2\nu)$ with μ being the shear modulus and ν the Poisson's ratio.

Depending on the given material property (e.g., isotropic material), the six eigenvalues of Eq. (11) may not be distinct. Should repeated roots occur, a slight change in the material constants would result in distinct roots with negligible errors.^{19,20} In doing so, the following simple solution structure can still be applied. Let us assume that the first three eigenvalues of Eq. (11) have positive imaginary parts, and the remaining three eigenvalues are conjugate to the first three, i.e., $p_{i+3} = \bar{p}_i$ ($i=1-3$). We distinguish the corresponding six eigenvectors by attaching a subscript to \mathbf{a} and \mathbf{b} . Then, the general solutions for the displacement and traction vectors (of the x_3 -dependent factor) are

$$\begin{bmatrix} \mathbf{u} \\ -i\mathbf{t} \end{bmatrix} = \begin{bmatrix} \mathbf{A} & \bar{\mathbf{A}} \\ \mathbf{B} & \bar{\mathbf{B}} \end{bmatrix} \begin{bmatrix} \langle e^{ip_1 x_3} \rangle & \mathbf{0} \\ \mathbf{0} & \langle e^{i\bar{p}_3 x_3} \rangle \end{bmatrix} \begin{bmatrix} \mathbf{K}_1 \\ \mathbf{K}_2 \end{bmatrix}, \quad (15)$$

where \mathbf{K}_1 and \mathbf{K}_2 are two constant vectors to be determined, and

$$\begin{aligned} \mathbf{A} &= [\mathbf{a}_1 \quad \mathbf{a}_2 \quad \mathbf{a}_3], \quad \mathbf{B} = [\mathbf{b}_1 \quad \mathbf{b}_2 \quad \mathbf{b}_3], \\ \langle e^{ip_1 x_3} \rangle &= \text{diag}[e^{ip_1 x_3} \quad e^{ip_2 x_3} \quad e^{ip_3 x_3}], \\ \text{Im}\{p_j\} &> 0 \quad (j=1-3). \end{aligned} \quad (16)$$

It is easy to show that the two matrices \mathbf{A} and \mathbf{B} satisfy the following normalized orthogonal relationship:¹⁶

$$\begin{bmatrix} \mathbf{B}^T & \mathbf{A}^T \\ \bar{\mathbf{B}}^T & \bar{\mathbf{A}}^T \end{bmatrix} \begin{bmatrix} \mathbf{A} & \bar{\mathbf{A}} \\ \mathbf{B} & \bar{\mathbf{B}} \end{bmatrix} = \begin{bmatrix} \mathbf{I} & \mathbf{0} \\ \mathbf{0} & \mathbf{I} \end{bmatrix}. \quad (17)$$

The above orthogonal relationship provides us with a simple way of inverting the eigenvector matrix, which is required in forming the transfer matrix.

Furthermore, in view of the above orthogonal relationship, we can also introduce the generalized Barnett-Lothe tensors \mathbf{S} , \mathbf{H} , \mathbf{L} defined by¹⁶

$$\mathbf{S} = i(2\mathbf{A}\mathbf{B}^T - \mathbf{I}), \quad \mathbf{H} = 2i\mathbf{A}\mathbf{A}^T, \quad \mathbf{L} = -2i\mathbf{B}\mathbf{B}^T, \quad (18)$$

with \mathbf{H} and \mathbf{L} being symmetric and positive definite and $\mathbf{S}\mathbf{H}$, $\mathbf{L}\mathbf{S}$, $\mathbf{H}^{-1}\mathbf{S}$, $\mathbf{S}\mathbf{L}^{-1}$ being antisymmetric. The generalized Barnett-Lothe tensors will be useful when addressing a semi-infinite medium. We further point out that, for isotropic materials, if we set

$$k_1 = \eta \cos \theta, \quad k_2 = \eta \sin \theta, \quad (19)$$

where η is the norm of (k_1, k_2) , and define the following three vectors:

$$\mathbf{x} = \begin{bmatrix} \sin \theta \\ -\cos \theta \\ 0 \end{bmatrix}, \quad \mathbf{n} = \begin{bmatrix} 0 \\ 0 \\ -1 \end{bmatrix}, \quad \mathbf{m} = \begin{bmatrix} \cos \theta \\ \sin \theta \\ 0 \end{bmatrix}, \quad (20)$$

then the three generalized Barnett-Lothe tensors can be reduced to¹⁶

$$\mathbf{S} = \frac{1-2\nu}{2(1-\nu)}(\mathbf{m}\mathbf{n}^T - \mathbf{n}\mathbf{m}^T),$$

$$\mathbf{H} = \frac{1}{4\eta\mu(1-\nu)}[(3-4\nu)\mathbf{I} + \mathbf{x}\mathbf{x}^T],$$

$$\mathbf{L} = \frac{\eta\mu}{1-\nu}(\mathbf{I} - \nu\mathbf{x}\mathbf{x}^T). \quad (21)$$

With the displacement and traction vectors in Eq. (15), the in-plane stress components can be expressed in terms of them as

$$\begin{bmatrix} \sigma_{11} \\ \sigma_{22} \\ \sigma_{12} \end{bmatrix} = i \left\{ \begin{bmatrix} k_1 c_{11} + k_2 c_{16} & k_1 c_{16} + k_2 c_{12} & k_1 c_{15} + k_2 c_{14} \\ k_1 c_{12} + k_2 c_{26} & k_1 c_{26} + k_2 c_{22} & k_1 c_{25} + k_2 c_{24} \\ k_1 c_{16} + k_2 c_{66} & k_1 c_{66} + k_2 c_{26} & k_1 c_{56} + k_2 c_{46} \end{bmatrix} \right. \\ \left. - \begin{bmatrix} c_{15} & c_{14} & c_{13} \\ c_{25} & c_{24} & c_{23} \\ c_{56} & c_{46} & c_{36} \end{bmatrix} \mathbf{T}^{-1} \mathbf{R}^T \right\} \mathbf{u} + \begin{bmatrix} c_{15} & c_{14} & c_{13} \\ c_{25} & c_{24} & c_{23} \\ c_{56} & c_{46} & c_{36} \end{bmatrix} \mathbf{T}^{-1} \mathbf{t}. \quad (22)$$

IV. TRANSFER MATRIX FOR THE $(N-1)$ THIN BONDED LAYERS

For a certain elastic layer k of finite thickness h_k with its lower surface at $x_3=z_{k-1}$ ($k=2,3,\dots,N$), it follows from Eqs. (15) and (17) that \mathbf{K}_1 and \mathbf{K}_2 can be expressed in terms of the displacement and traction vectors at its lower interface $x_3=z_{k-1}$ as

$$\begin{bmatrix} \mathbf{K}_1 \\ \mathbf{K}_2 \end{bmatrix} = \begin{bmatrix} \langle e^{-i\bar{p}\alpha z_{k-1}} \rangle & \mathbf{0} \\ \mathbf{0} & \langle e^{-i\bar{p}\alpha z_{k-1}} \rangle \end{bmatrix} \begin{bmatrix} \mathbf{B}^T & \mathbf{A}^T \\ \bar{\mathbf{B}}^T & \bar{\mathbf{A}}^T \end{bmatrix} \begin{bmatrix} \mathbf{u} \\ -i\mathbf{t} \end{bmatrix}_{z_{k-1}}. \quad (23)$$

Then, the displacement and traction vectors at any position within this layer are related to the displacement and traction vectors at its lower interface $x_3=z_{k-1}$ as follows:

$$\begin{bmatrix} \mathbf{u} \\ -i\mathbf{t} \end{bmatrix} = \mathbf{E}_k(x_3 - z_{k-1}) \begin{bmatrix} \mathbf{u} \\ -i\mathbf{t} \end{bmatrix}_{z_{k-1}}, \quad (24)$$

where

$$\mathbf{E}_k(x_3) = \begin{bmatrix} \mathbf{A} & \bar{\mathbf{A}} \\ \mathbf{B} & \bar{\mathbf{B}} \end{bmatrix} \begin{bmatrix} \langle e^{i\bar{p}\alpha x_3} \rangle & \mathbf{0} \\ \mathbf{0} & \langle e^{i\bar{p}\alpha x_3} \rangle \end{bmatrix} \begin{bmatrix} \mathbf{B}^T & \mathbf{A}^T \\ \bar{\mathbf{B}}^T & \bar{\mathbf{A}}^T \end{bmatrix} \quad (25)$$

is called the transfer matrix (or the propagator matrix).¹⁹ In deriving the above expression of $\mathbf{E}_k(x_3)$, the orthogonal relationship in Eq. (17) has been utilized. Moreover, by utilizing the orthogonal relationships in Eqs. (17) and (11), the transfer matrix $\mathbf{E}_k(x_3)$ can also be expressed in terms of a matrix exponential as

$$\mathbf{E}_k(x_3) = \exp(i\mathbf{N}x_3), \quad (26)$$

which is strikingly simple and can be easily calculated even the matrix \mathbf{N} is nonsemisimple when the material is (mathematically) degenerate such as an isotropic material.¹⁶ Equation (26) demonstrates that by employing the matrix exponential for the transfer matrix, one can avoid directly solving the eigenvalue problem of Eq. (11).

It follows from Eq. (24) that the displacement and traction vectors at the upper interface $x_3=z_k$ of layer k is related to those at the lower interface $x_3=z_{k-1}$ through the following propagating relation:

$$\begin{bmatrix} \mathbf{u} \\ -i\mathbf{t} \end{bmatrix}_{z_k} = \mathbf{E}_k(h_k) \begin{bmatrix} \mathbf{u} \\ -i\mathbf{t} \end{bmatrix}_{z_{k-1}}. \quad (27)$$

Consequently, the solution at the interface $x_3=z_n^-$ (here the superscript “-” indicates approaching the interface from below) of the multilayered system can be expressed by that at the bottom interface $x_3=0$ as

$$\begin{bmatrix} \mathbf{u} \\ -i\mathbf{t} \end{bmatrix}_{z_n^-} = \begin{bmatrix} \mathbf{Y}_{11} & \mathbf{Y}_{12} \\ \mathbf{Y}_{21} & \mathbf{Y}_{22} \end{bmatrix} \begin{bmatrix} \mathbf{u} \\ -i\mathbf{t} \end{bmatrix}_0, \quad (28)$$

where \mathbf{Y}_{11} , \mathbf{Y}_{12} , \mathbf{Y}_{21} , \mathbf{Y}_{22} are four 3×3 matrices given by

$$\begin{bmatrix} \mathbf{Y}_{11} & \mathbf{Y}_{12} \\ \mathbf{Y}_{21} & \mathbf{Y}_{22} \end{bmatrix} = \mathbf{E}_n(h_n) \times \mathbf{E}_{n-1}(h_{n-1}) \times \dots \times \mathbf{E}_3(h_3) \times \mathbf{E}_2(h_2). \quad (29)$$

Similarly, the solution at the top interface $x_3=H$ of the multilayered system can be expressed by that at the interface $x_3=z_n^+$ (here the superscript “+” indicates approaching the interface from above) as

$$\begin{bmatrix} \mathbf{u} \\ -i\mathbf{t} \end{bmatrix}_H = \begin{bmatrix} \tilde{\mathbf{Y}}_{11} & \tilde{\mathbf{Y}}_{12} \\ \tilde{\mathbf{Y}}_{21} & \tilde{\mathbf{Y}}_{22} \end{bmatrix} \begin{bmatrix} \mathbf{u} \\ -i\mathbf{t} \end{bmatrix}_{z_n^+}, \quad (30)$$

where $\tilde{\mathbf{Y}}_{11}$, $\tilde{\mathbf{Y}}_{12}$, $\tilde{\mathbf{Y}}_{21}$, $\tilde{\mathbf{Y}}_{22}$ are four 3×3 matrices given by

$$\begin{bmatrix} \tilde{\mathbf{Y}}_{11} & \tilde{\mathbf{Y}}_{12} \\ \tilde{\mathbf{Y}}_{21} & \tilde{\mathbf{Y}}_{22} \end{bmatrix} = \mathbf{E}_N(h_N) \times \mathbf{E}_{N-1}(h_{N-1}) \times \dots \times \mathbf{E}_{n+2}(h_{n+2}) \times \mathbf{E}_{n+1}(h_{n+1}). \quad (31)$$

V. GENERAL SOLUTION FOR THE TWO SEMI-INFINITE MEDIA

Since $x_3 \rightarrow -\infty$ for the bottom semi-infinite medium, the solution for the bottom semi-infinite medium can be taken as

$$\begin{bmatrix} \mathbf{u} \\ -i\mathbf{t} \end{bmatrix} = 2i \begin{bmatrix} \bar{\mathbf{A}}_{(1)} \\ \bar{\mathbf{B}}_{(1)} \end{bmatrix} \langle e^{i\bar{p}\alpha(1)x_3} \rangle \bar{\mathbf{B}}_{(1)}^T \mathbf{q}_b, \quad (32)$$

where \mathbf{q}_b is a constant vector to be determined and the subscript “(1)” is utilized to indicate the quantities associated with the bottom semi-infinite medium 1. The above general solution ensures that the elastic field approaches zero as $x_3 \rightarrow -\infty$.

Similarly, due to the fact that $x_3 \rightarrow +\infty$ for the top semi-infinite medium, then the general solution for the top semi-infinite medium can be taken as

$$\begin{bmatrix} \mathbf{u} \\ -i\mathbf{t} \end{bmatrix} = 2i \begin{bmatrix} \mathbf{A}_{(N+1)} \\ \mathbf{B}_{(N+1)} \end{bmatrix} \langle e^{i\bar{p}\alpha(N+1)(x_3-H)} \rangle \mathbf{B}_{(N+1)}^T \mathbf{q}_u, \quad (33)$$

where \mathbf{q}_u is a constant vector to be determined and the subscript “(N+1)” is utilized to indicate the quantities associated with the top semi-infinite medium N+1. The above general solution ensures that the elastic field approaches zero as $x_3 \rightarrow +\infty$.

VI. SOLUTION OF THE TOTAL STRUCTURE

Enforcing that the displacements and tractions are continuous across the bottom interface $x_3=0$, it follows from Eqs. (28) and (32) that we can arrive at the following relationship between the traction and displacement vectors at the interface $x_3=z_n^-$:

$$\mathbf{t}(z_n^-) = i[\mathbf{Y}_{21}(i\mathbf{I} - \mathbf{S}_{(1)}) + \mathbf{Y}_{22}\mathbf{L}_{(1)}][\mathbf{Y}_{11}(i\mathbf{I} - \mathbf{S}_{(1)}) + \mathbf{Y}_{12}\mathbf{L}_{(1)}]^{-1}\mathbf{u}(z_n^-). \quad (34)$$

During the derivation of the above expression, Eq. (18) for the generalized Barnett-Lothe tensors has been utilized.

Similarly, due to the fact that the displacements and tractions are also continuous across top the interface $x_3=H$, then it follows from Eqs. (30) and (33) that we can arrive at the

following relationship between the traction and displacement vectors at the interface $x_3 = z_n^+$:

$$\begin{aligned} \mathbf{t}(z_n^+) = & -i[\tilde{\mathbf{Y}}_{12} + (\mathbf{S}_{(N+1)} + i\mathbf{I})\mathbf{L}_{(N+1)}^{-1}\tilde{\mathbf{Y}}_{22}]^{-1}[\tilde{\mathbf{Y}}_{11} + (\mathbf{S}_{(N+1)} \\ & + i\mathbf{I})\mathbf{L}_{(N+1)}^{-1}\tilde{\mathbf{Y}}_{21}]\mathbf{u}(z_n^+). \end{aligned} \quad (35)$$

In view of Eq. (1) for the double Fourier series, the boundary conditions on the interface $x_3 = z_n$ can be recast into

$$\mathbf{t}(z_n^+) = \mathbf{t}(z_n^-), \quad \mathbf{u}(z_n^+) - \mathbf{u}(z_n^-) = \mathbf{\Delta}, \quad (36)$$

where

$$\mathbf{\Delta} = [\Delta_1^{(G)} \quad \Delta_2^{(G)} \quad \Delta_3^{(G)}]^T. \quad (37)$$

Consequently, it follows from Eqs. (34)–(36) that the displacement and traction vectors at $x_3 = z_n$ can be uniquely determined as

$$\begin{aligned} \mathbf{u}(z_n^-) &= -\mathbf{\Omega}^{-1}\mathbf{\Delta}, \\ \mathbf{u}(z_n^+) &= (\mathbf{I} - \mathbf{\Omega}^{-1})\mathbf{\Delta}, \\ \mathbf{t}(z_n^+) = \mathbf{t}(z_n^-) &= -i[\mathbf{Y}_{21}(i\mathbf{I} - \mathbf{S}_{(1)}) + \mathbf{Y}_{22}\mathbf{L}_{(1)}] \\ &\times [\mathbf{Y}_{11}(i\mathbf{I} - \mathbf{S}_{(1)}) + \mathbf{Y}_{12}\mathbf{L}_{(1)}]^{-1}\mathbf{\Omega}^{-1}\mathbf{\Delta}, \end{aligned} \quad (38)$$

where

$$\begin{aligned} \mathbf{\Omega} = & \mathbf{I} + [\tilde{\mathbf{Y}}_{11} + (\mathbf{S}_{(N+1)} + i\mathbf{I})\mathbf{L}_{(N+1)}^{-1}\tilde{\mathbf{Y}}_{21}]^{-1}[\tilde{\mathbf{Y}}_{12} + (\mathbf{S}_{(N+1)} \\ & + i\mathbf{I})\mathbf{L}_{(N+1)}^{-1}\tilde{\mathbf{Y}}_{22}][\mathbf{Y}_{21}(i\mathbf{I} - \mathbf{S}_{(1)}) + \mathbf{Y}_{22}\mathbf{L}_{(1)}] \\ & \times [\mathbf{Y}_{11}(i\mathbf{I} - \mathbf{S}_{(1)}) + \mathbf{Y}_{12}\mathbf{L}_{(1)}]^{-1}. \end{aligned} \quad (39)$$

Once the displacement and traction vectors are known at the interface $x_3 = z_n$, the displacement and traction vectors at any position within layer k ($2 \leq k \leq N$) of the layered system can be conveniently determined as

$$\begin{aligned} \begin{bmatrix} \mathbf{u} \\ -i\mathbf{t} \end{bmatrix} &= \mathbf{E}_k(x_3 - z_{k-1}) \times \mathbf{E}_{k-1}(h_{k-1}) \times \cdots \times \mathbf{E}_3(h_3) \\ &\times \mathbf{E}_2(h_2) \times \begin{bmatrix} \mathbf{Y}_{11} & \mathbf{Y}_{12} \\ \mathbf{Y}_{21} & \mathbf{Y}_{22} \end{bmatrix}^{-1} \begin{bmatrix} \mathbf{u} \\ -i\mathbf{t} \end{bmatrix}_{z_n^-} \\ &= \mathbf{E}_k(x_3 - z_{k-1}) \times \mathbf{E}_k(-h_k) \times \mathbf{E}_{k+1}(-h_{k+1}) \\ &\times \mathbf{E}_{n-1}(-h_{n-1}) \times \mathbf{E}_n(-h_n) \begin{bmatrix} \mathbf{u} \\ -i\mathbf{t} \end{bmatrix}_{z_n^-} \\ &\text{for } 2 \leq k \leq n \quad \text{and } z_{k-1} < x_3 < z_k, \end{aligned} \quad (40)$$

$$\begin{aligned} \begin{bmatrix} \mathbf{u} \\ -i\mathbf{t} \end{bmatrix} &= \mathbf{E}_k(x_3 - z_{k-1}) \times \mathbf{E}_{k-1}(h_{k-1}) \times \cdots \times \mathbf{E}_{n+2}(h_{n+2}) \\ &\times \mathbf{E}_{n+1}(h_{n+1}) \begin{bmatrix} \mathbf{u} \\ -i\mathbf{t} \end{bmatrix}_{z_n^+} \quad \text{for } n+1 \leq k \leq N \\ &\text{and } z_{k-1} < x_3 < z_k. \end{aligned} \quad (41)$$

Similarly, the displacement and traction vectors at any position within the bottom semi-infinite anisotropic medium are given by

$$\begin{aligned} \begin{bmatrix} \mathbf{u} \\ -i\mathbf{t} \end{bmatrix} &= 2i \begin{bmatrix} \bar{\mathbf{A}}_{(1)} \\ \bar{\mathbf{B}}_{(1)} \end{bmatrix} \langle e^{i\bar{p}\alpha(1)x_3} \rangle \bar{\mathbf{B}}_{(1)}^T [\mathbf{Y}_{11}(i\mathbf{I} - \mathbf{S}_{(1)}) \\ &+ \mathbf{Y}_{12}\mathbf{L}_{(1)}]^{-1} \mathbf{u}(z_n^-), \quad x_3 < 0, \end{aligned} \quad (42)$$

and the displacement and traction vectors at any position within the top semi-infinite anisotropic medium are given by

$$\begin{aligned} \begin{bmatrix} \mathbf{u} \\ -i\mathbf{t} \end{bmatrix} &= 2i \begin{bmatrix} \mathbf{A}_{(N+1)} \\ \mathbf{B}_{(N+1)} \end{bmatrix} \langle e^{ip\alpha(N+1)(x_3-H)} \rangle \mathbf{B}_{(N+1)}^T (\mathbf{S}_{(N+1)} + i\mathbf{I})^{-1} \\ &\times [\tilde{\mathbf{Y}}_{11} \quad \tilde{\mathbf{Y}}_{12}] \begin{bmatrix} \mathbf{u} \\ -i\mathbf{t} \end{bmatrix}_{z_n^+}, \quad x_3 > H. \end{aligned} \quad (43)$$

Once the displacement and traction vectors are known, the distributions of the in-plane stresses σ_{11} , σ_{22} , and σ_{12} can be determined through Eq. (22).

For $\mathbf{G} = \mathbf{0}$, the corresponding displacements are constant within each layer. In addition, the constant displacements are common for each layer due to the fact that $\Delta_k^{(G=0)} = 0$ and therefore, can be chosen arbitrarily. For example, they can be chosen to maintain $(0, 0, z_n)$ as a fixed point. Finally, we can add together the results for different values of zero and non-zero values of \mathbf{G} .

VII. MAIN FEATURES OF THE METHODOLOGY

The main features of the methodology presented in this work are as follows.

(i) One needs only to invert several 3×3 matrices to arrive at the displacement and traction vectors at any position within the anisotropic multilayered crystal [see Eqs. (38)–(43)]. Thus, it is very suitable to address a crystal composed of an arbitrarily large number of layers. Due to the time saved, then it becomes feasible, by summing enough terms of the double Fourier series, to calculate the stress field close to the interface where the array of misfit dislocations is located. It is a great advance compared to the existing method, which is rather formidable and time consuming as it requires inverting a $6N \times 6N$ matrix for a multilayered structure with N interfaces. The earlier approach is particularly difficult when the value of N is very large (say, a hundred layers).

(ii) When letting $k_2 = 0$ (or $k_1 = 0$), the derived solution can also be used to investigate the periodic problem in the x_1 (or x_2) direction. One example is a multilayered system containing an array of periodic misfit dislocations with Burgers vector $\hat{\mathbf{b}} = (\hat{b}_1, \hat{b}_2, \hat{b}_3)$ along the planar interface $x_3 = z_n$.⁹ In this case, the 3D problem is reduced to a 2D one in which the solutions are independent of the x_2 (or the x_1) coordinate.

(iii) The solution of the eigenvalue problem [Eq. (11)] for the $(N-1)$ thin layers can be circumvented due to the fact that the transfer matrix can be expressed in terms of the matrix exponential [Eq. (25)]. As a result, each thin layer can be made of either anisotropic material or the mathematically degenerated isotropic material. In general, the eigenvalue problem [Eq. (11)] has to be solved for the two semi-infinite media since there is no such a concept of transfer matrix for

a semi-infinite medium. On the other hand, if the explicit expressions of the generalized Barnett-Lothe tensors \mathbf{S} , \mathbf{H} , and \mathbf{L} are known for the involved material like the isotropic case [see Eq. (21)], then even the solution of the eigenvalue problem [Eq. (11)] for the two semi-infinite media is *unnecessary* if one is interested in the elastic fields in the welded $(N-1)$ thin layers. In this special case, the elastic fields in the thin layers are completely determined by the transfer matrices \mathbf{Y}_{ij} , $\tilde{\mathbf{Y}}_{ij}$ ($i, j=1, 2$) and the generalized Barnett-Lothe tensors $\mathbf{S}_{(1)}$, $\mathbf{L}_{(1)}$, $\mathbf{S}_{(N+1)}$, $\mathbf{L}_{(N+1)}$ [see Eqs. (38)–(41)].

(iv) Should there be any thick layer in the layered system, the corresponding transfer matrix can be normalized using the method proposed by Pan.¹⁷ Furthermore, to accelerate the convergence of the Fourier series for observation points close to the dislocation segment, the explicit solution to the corresponding homogeneous space can be utilized so that the singular and slow convergent part can be analytically treated.²¹

VIII. APPLICATION

To verify the correctness and to show the power of the method, we first consider a multilayered structure with $N=5$, formed by four thin alternating GaAs and Si layers sandwiched between two semi-infinite media GaAs and Si. This problem was discussed by Bonnet⁹ when the six alternating media were assumed to be isotropic. The thickness of each layer is 2 nm and, as a result, the five interfaces are located at $x_3=0, 2, 4, 6, 8$ nm. We consider the problem of a single array of periodic edge misfit dislocations with Burgers vector $\hat{\mathbf{b}}=(\hat{b}_1, \hat{b}_2, \hat{b}_3)=(0.3838 \text{ nm}, 0, 0)$ located along the central interface $x_3=4$ nm. The result is a sawtooth change of misfit displacement $\Delta u_k = u_k^{(n+1)} - u_k^{(n)}$ ($n=3$) along the interface, which can be expanded into Fourier series.⁹ The period Λ of the misfit dislocations is 9.7 nm. In addition, the misfit dislocations are infinitely long in the x_2 direction. As a result, the problem is 2D in which the solutions are independent of the x_2 coordinate. Furthermore, we take $k_1=2\pi m/\Lambda$ with m being a nonzero integer and $k_2=0$ in our formulation. We calculate the in-plane stress component σ_{11} and the traction component σ_{33} along the x_3 axis ($x_1=0$). First, as in Ref. 9, we assume that both GaAs and Si are isotropic with elastic constants $\mu_{\text{GaAs}}=46.01$ GPa, $\nu_{\text{GaAs}}=0.24$, $\mu_{\text{Si}}=66.11$ GPa, $\nu_{\text{Si}}=0.23$. The distributions of σ_{11} and σ_{33} along the x_3 axis when each medium is isotropic are illustrated as dashed lines in Figs. 2 and 3, and the values of σ_{11} on the two sides of the interfaces $x_3=0, 2, 6, 8$ nm are given in the second row of Table I. It is observed that the present method based on the Stroh formalism and transfer matrix produces exactly the same the results as in Bonnet.⁹ Consequently, the correctness of the method is verified.

It is well known that both GaAs and Si are elastically anisotropic (cubic) with elastic constants $c_{11}=118$ GPa, $c_{12}=53.5$ GPa, $c_{44}=59.4$ GPa for GaAs and $c_{11}=165.7$ GPa, $c_{12}=63.9$ GPa, $c_{44}=79.6$ GPa for Si.^{9,13,14} Therefore, it would be interesting to study the influence of material anisotropy on the misfit dislocation-induced field. The distributions of σ_{11} and σ_{33} along the x_3 axis when each medium is

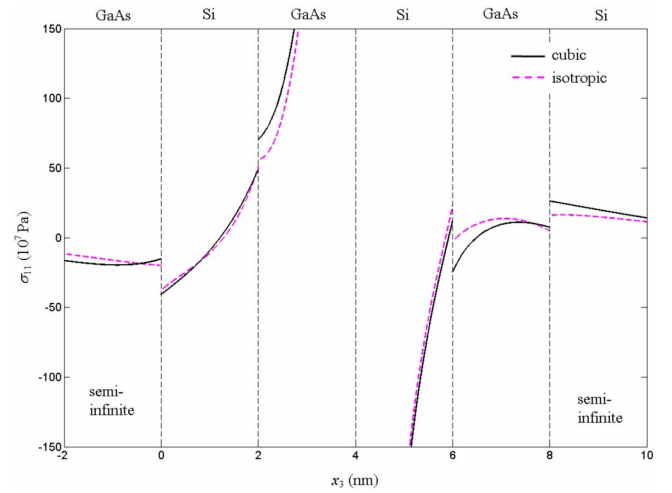


FIG. 2. (Color online) Distribution of the in-plane stress σ_{11} along the x_3 axis ($x_1=0$) for a $(N=5)$ multilayered structure formed by alternating GaAs and Si. The misfit dislocation array lies at the interface $x_3=4$ nm and is infinitely long in the x_2 direction. The dark solid lines are the results when GaAs and Si are taken to be cubic and the pink dashed lines are the corresponding results when GaAs and Si are assumed to be isotropic.

anisotropic (cubic) are illustrated as solid lines in Figs. 2 and 3 and the values of σ_{11} on the two sides of the interfaces $x_3=0, 2, 6,$ and 8 nm are further listed in the third row of Table I for comparison with the corresponding isotropic case. Clearly, both σ_{11} and σ_{33} based on the true anisotropic (cubic) material model are significantly different from the corresponding results when each medium is simplified to be isotropic. As such, the effect of semiconductor anisotropy on

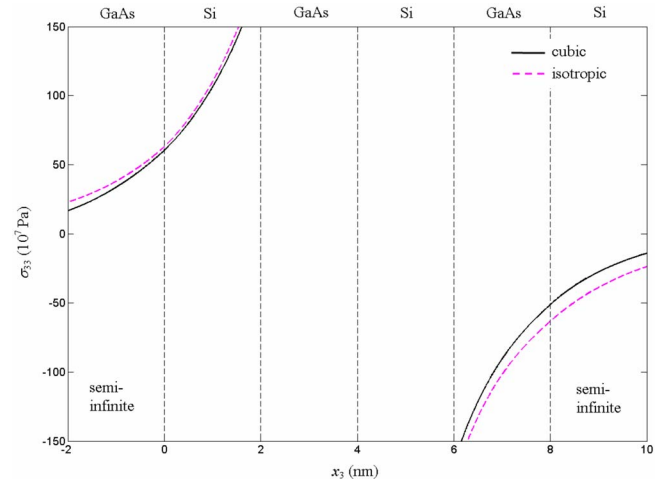


FIG. 3. (Color online) Distribution of the traction component σ_{33} along the x_3 axis ($x_1=0$) for a $(N=5)$ multilayered system formed by alternating GaAs and Si. The misfit dislocation array lies at the interface $x_3=4$ nm and is infinitely long in the x_2 direction. The dark solid lines are the results when GaAs and Si are taken to be cubic and the pink dashed lines are the corresponding results when GaAs and Si are assumed to be isotropic.

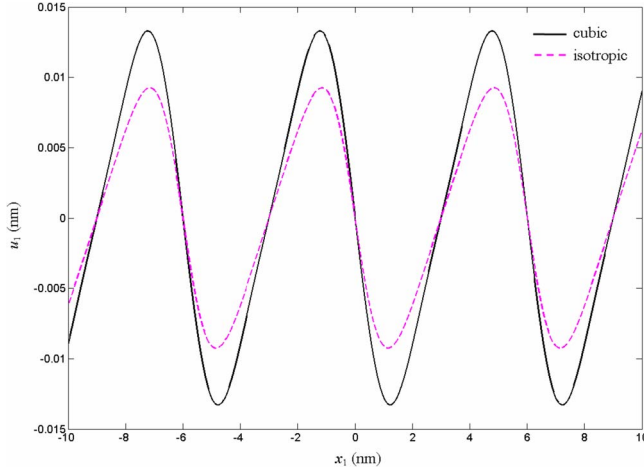


FIG. 4. (Color online) Periodic distribution of the horizontal displacement u_1 along the traction-free surface of the InAs thin film bonded to the GaAs substrate. The misfit dislocation array lies at the InAs/GaAs interface. The dark solid line is the result when both the InAs thin film and GaAs substrate are taken to be cubic, whereas the pink dashed line is the corresponding result when both InAs and GaAs are assumed to be isotropic.

the misfit dislocation-induced stresses should be taken into consideration for more accurate modeling of the multilayer GaAs/Si.

Next, we consider an edge misfit dislocation array with Burgers vector $\hat{\mathbf{b}}=(\hat{b}_1, \hat{b}_2, \hat{b}_3)=(0.2 \text{ nm}, 0, 0)$ and the period $\Lambda=6 \text{ nm}$ along the heterointerface between the InAs ($c_{11}=83.29 \text{ GPa}$, $c_{12}=45.26 \text{ GPa}$, $c_{44}=39.59 \text{ GPa}$) thin film of thickness $h=2 \text{ nm}$ and GaAs substrate with its cubic material properties given above. In this case, $N=2$. We illustrate in Figs. 4 and 5 the induced horizontal displacement u_1 and vertical displacement u_3 along the traction-free surface of the InAs thin film. The solid lines in Figs. 4 and 5 are the results when both the InAs thin film and GaAs substrate are taken to be anisotropic (cubic), whereas the dashed lines are the corresponding results when they are assumed to be isotropic (with $c_{11}=c_{12}+2c_{44}$). Once again, we observe that the isotro-

TABLE I. Values of σ_{11} on the two sides of each interface of the multilayer GaAs/Si/GaAs/Si/GaAs/Si with $N=5$. The interface locations are denoted by x_3 . Two material cases are studied: elastically isotropic (assumed for demonstration purposes) and elastically cubic (true). The values in the parentheses in the second row are the results of Bonnet (Ref. 9).

x_3 (nm)	0	2	6	8
(isotropic)	-19.9/-37.7	51.0/56.5	23.0/-2.71	4.65/16.1
σ_{11} (10^7 Pa)	(-19.9/-37.7)	(50.8/56.5)	(23.0/-2.6)	(4.7/16.1)
(cubic)	-15.2/-40.8	49.1/70.4	12.2/-24.5	7.37/26.3
σ_{11} (10^7 Pa)				

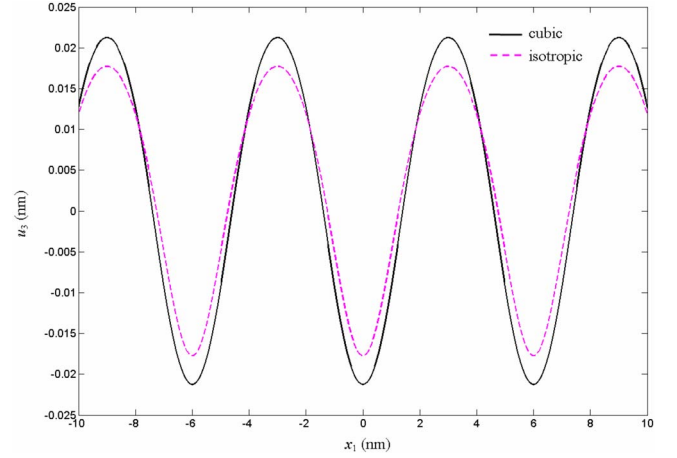


FIG. 5. (Color online) Periodic distribution of the horizontal displacement u_3 along the traction-free surface of the InAs thin film bonded to the GaAs substrate. The misfit dislocation array lies at the InAs/GaAs interface. The dark solid line is the result when both the InAs thin film and GaAs substrate are taken to be cubic, whereas the pink dashed line is the corresponding result when both InAs and GaAs are assumed to be isotropic.

pic assumption for the thin film and substrate could cause considerable error in displacement distribution. Therefore, our model, which includes the traction-free surface, semiconductor anisotropy, and misfit dislocation interaction among adjacent dislocations, can be combined with experimental measurements to accurately characterize the misfit dislocation-induced elastic field in thin-film and superlattice structures.²²

IX. CONCLUSIONS

We have developed an efficient computational method based on double Fourier series expansion, the Stroh formalism, and transfer matrix method for calculating the elastic field associated with a semiconductor system composed of an arbitrary number of thin bonded homogeneous and anisotropic elastic layers, sandwiched between two anisotropic semi-infinite media. One interface of the multilayered crystal contains a biperiodic array of misfit dislocations. The formulations presented are strikingly simple in that once the 6×6 matrix \mathbf{N} for each thin elastic layer and the Barnett-Lothe tensors \mathbf{L} and \mathbf{S} for the two semi-infinite media are determined, the displacement and traction vectors (and as a result the in-plane stresses) can be conveniently obtained. Numerical results show that the new method is correct and powerful and that material anisotropy can significantly influence the misfit dislocation-induced physical quantities.

ACKNOWLEDGMENTS

This work was supported in part by AFOSR FA9550-06-1-0317. The authors would also like to thank Roland Bonnet for his constructive comments.

- ¹L. Sorba, G. Bratina, A. Franciosi, L. Tapfer, G. Scamarcio, V. Spagnolo, and E. Molinari, *Appl. Phys. Lett.* **61**, 1570 (1992); G. Scamarcio, V. Spagnolo, E. Molinari, L. Tapfer, L. Sorba, G. Bratina, and A. Franciosi, *Phys. Rev. B* **46**, 7296 (1992).
- ²*Wafer Bonding: Applications and Technology*, edited by M. Alexe and U. Goesele (Springer-Verlag, Berlin, 2004).
- ³J. S. Koehler, *Phys. Rev. B* **2**, 547 (1970).
- ⁴P. Anderson, *Scr. Metall. Mater.* **27**, 687 (1992).
- ⁵D. S. Lashmore and R. Thomson, *J. Mater. Res.* **7**, 2379 (1992).
- ⁶X. G. Ning, D. S. Wilkinson, J. F. Mao, J. H. Li, H. Q. He, Z. J. Pu, and D. X. Zou, *Mater. Sci. Forum* **207-209**, 313 (1996).
- ⁷W. Cai, V. V. Bulatov, J. Chang, J. Li, and S. Yip, *Phys. Rev. Lett.* **86**, 5727 (2001); W. Cai, V. V. Bulatov, J. Chang, J. Li, and S. Yip, *Philos. Mag.* **83**, 539 (2003); J. Li, C. Wang, J. Chang, W. Cai, V. V. Bulatov, K. Ho, and S. Yip, *Phys. Rev. B* **70**, 104113 (2004).
- ⁸H. Bougrab, K. Inal, H. Sabar, and M. Berveiller, *J. Appl. Crystallogr.* **37**, 270 (2004).
- ⁹R. Bonnet, *Phys. Rev. B* **53**, 10 978 (1996).
- ¹⁰R. Benbouda, A. Mihi, M. Brioua, S. Madani, and L. Adami, *Phys. Status Solidi A* **202**, 2462 (2005).
- ¹¹R. Bonnet, *Interface Sci.* **4**, 169 (1997).
- ¹²R. Bonnet, *Phys. Status Solidi A* **180**, 487 (2000).
- ¹³T. Outtas, L. Adami, A. Derardja, S. Madani, and R. Bonnet, *Phys. Status Solidi A* **188**, 1041 (2001).
- ¹⁴T. Outtas, L. Adami, and R. Bonnet, *Solid State Sci.* **4**, 161 (2002).
- ¹⁵D. M. Barnett and J. Lothe, *Phys. Norv.* **8**, 13 (1975).
- ¹⁶T. C. T. Ting, *Anisotropic Elasticity: Theory and Applications* (Oxford University Press, New York 1996).
- ¹⁷E. Pan, *Appl. Math. Model.* **21**, 509 (1997).
- ¹⁸B. Yang and E. Pan, *Eng. Anal. Boundary Elem.* **26**, 355 (2002).
- ¹⁹E. Pan, *Chin. J. Mech., Ser. A* **19**, 127 (2003).
- ²⁰E. Pan, *Eng. Anal. Boundary Elem.* **23**, 67 (1999).
- ²¹E. Pan, B. Yang, G. Cai, and F. G. Yuan, *Eng. Anal. Boundary Elem.* **25**, 31 (2001).
- ²²R. Stalder, H. Sirringhaus, N. Onda, and H. Von Kanel *Appl. Phys. Lett.* **59**, 1960 (1991); J. G. Belk, D. W. Pashley, B. A. Joyce, and T. S. Jones, *Phys. Rev. B* **58**, 16194 (1998); T. D. Yong, J. Kioseoglou, G. P. Dimitrakopoulos, P. Dluzewski, and P. Komninou, *J. Phys. D* **40**, 4084 (2007).